NANO LETTERS

Letter

pubs.acs.org/NanoLett

Direct Identification of Metallic and Semiconducting Single-Walled Carbon Nanotubes in Scanning Electron Microscopy

Jie Li, Yujun He, Yimo Han, Kai Liu,† Jiaping Wang, Qunqing Li, Shoushan Fan, and Kaili Jiang*

State Key Laboratory of Low-Dimensional Quantum Physics, Department of Physics & Tsinghua-Foxconn Nanotechnology Research Center, Tsinghua University, Beijing 100084, China

ABSTRACT: Because of their excellent electrical and optical properties, carbon nanotubes have been regarded as extremely promising candidates for high-performance electronic and optoelectronic applications. However, effective and efficient distinction and separation of metallic and semiconducting single-walled carbon nanotubes are always challenges for their practical applications. Here we show that metallic and semiconducting single-walled carbon nanotubes on SiO_2 can have obviously different contrast in scanning electron microscopy due to their conductivity difference and thus can be effectively and efficiently identified. The correlation between conductivity and contrast difference has been confirmed by using voltage-contrast scanning electron microcopy, peak force tunneling atom force microscopy, and field effect transistor testing. This phenomenon can be understood via a proposed mechanism involving the e-beam-induced surface potential of insulators and the conductivity difference between metallic and semiconducting SWCNTs. This method demonstrates great promise to achieve rapid and large-scale distinguishing between metallic and semiconducting single-walled carbon nanotubes, adding a new function to conventional SEM.

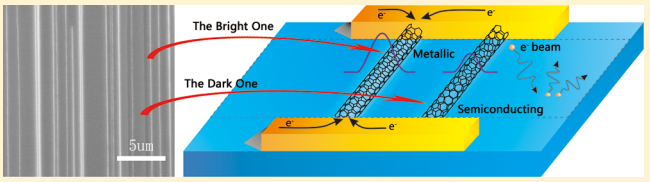

KEYWORDS: *Carbon nanotube, identification, metallic, semiconducting, scanning electron microscopy*

Single-walled carbon nanotubes (SWCNTs) can be metallic or semiconducting depending on their chiral angles.[1,2] Metallic SWCNTs can serve as effective nanometer sized wires or electrodes[3−5] and have potential applications in transparent conducting films as well as interconnects for integrated circuits (ICs).[6] Semiconducting SWCNTs can be used as conductive channels of field effect transistors (FET) with high ON/OFF ratios for logic device applications.[7−10] Both kinds of SWCNTs have to be of high purity for the aforementioned applications. Unfortunately, the as-synthesized SWCNTs are always a mixture of metallic and semiconducting tubes. Now the challenges are (1) developing an effective and efficient method of identifying metallic and semiconducting SWCNTs and then (2) developing the corresponding separation methods. To date, some methods have been developed to identify the types of SWCNTs, such as field effect transistor (FET) testing,[7] Raman spectroscopy,[1,11−13] and electrostatic force microscopy.[14−16] However, the most convenient and efficient facility for characterizing SWCNTs is scanning electron microcopy (SEM), which possesses the merits of rapid and large area imaging. Here we show that the contrast of SEM images has a relationship with the electrical properties of SWCNTs, which enables direct and efficient identification of metallic and semiconducting SWCNTs, adding a new function to conventional SEM.

In our experiment, horizontally aligned and high-density SWCNT arrays synthesized via chemical vapor deposition (CVD) on a stable temperature-cut (ST-cut) quartz substrate were used. A similar growth procedure can be found in published literatures.[17−22] After ST-cut quartz wafers were annealed at 900 °C in O_2 for 8 h, an Fe film with a nominal thickness of 0.2 nm used as catalyst precursor was patterned on the wafers. By annealing the quartz wafers at 700 °C in air, residue photoresist was removed and iron oxide nanoparticles were formed. After purging with argon (1000 sccm) at 700 °C for 10 min, the furnace was heated to 850 °C and a flow of argon (500 sccm) and hydrogen (500 sccm) was introduced into the system at the same time. The CVD growth of SWCNTs was implemented with a flow of methane (500 sccm), hydrogen (100 sccm), and argon (400 sccm) at 850 °C for 15 min. Then argon (1000 sccm) was introduced for flushing the chamber to end the growth process. The as-grown carbon nanotubes are all SWCNTs and are around 100 μm in length and 1.0−2.5 nm in diameter. Most of the SWCNTs have a diameter of 1.6−2.0 nm.

Figure 1a is a typical SEM (FEI Sirion 200, operated at 1 kV, a line scan time of 40 ms, 1936 lines per frame, spot size 4, final lens strip aperture size 100 μm) image of SWCNT arrays synthesized on a quartz substrate. The SEM image of the as-synthesized SWCNTs at higher magnification clearly shows that some tubes are very bright while the others are much darker (Figure 1b,c). Now the question is what the implication of the contrast difference is.

Considering the as-synthesized SWCNTs are a mixture of metallic and semiconducting tubes, we conjecture that the contrast difference might originate from the different conductivity of the tubes. To verify this hypothesis, we

Received: April 25, 2012
Revised: June 20, 2012
Published: June 25, 2012

   dx.doi.org/10.1021/nl301561f | *Nano Lett.* 2012, 12, 4095−4101

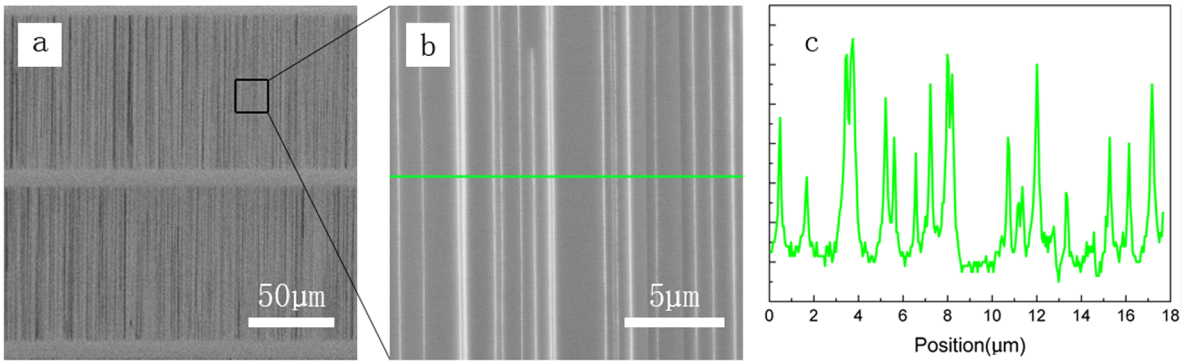

Figure 1. SEM images of horizontally aligned arrays grown on single-crystal quartz surface (a) at low magnification and (b) at high magnification, where contrast difference can be clearly discerned. (c) Gray level versus position extracted from (b) along the green line.

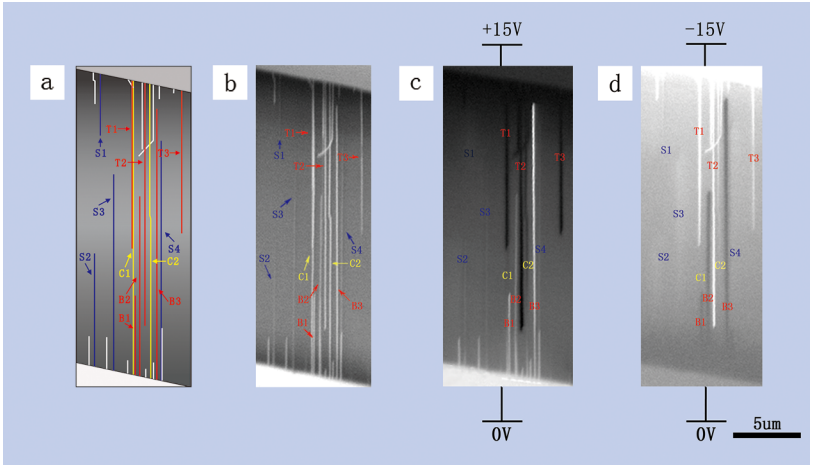

Figure 2. SEM images of SWCNTs at different voltage conditions: (a) schematic illustration of all the SWCNTs; (b) SEM images of SWCNTs without applying voltage; (c) SEM images of SWCNTs when apply 15 V voltage difference between the upper and lower electrode; (d) SEM images of SWCNTs when apply −15 V voltage difference between the upper and lower electrode.

designed and conducted a series of experiments, which will be discussed below in detail.

Typically, SEM images are acquired by detecting the intensity of secondary electrons knocked out from the sample by the primary electron beam; here we ignore the back-scattering electrons' contribution because a low accelerating voltage (1 kV) is used in our experiment. SEM image is therefore sensitive to the surface potential of the sample, which is known as the voltage contrast.[23] If we apply a voltage on the CNT samples, metallic CNTs will possess identical electric potential with the electrodes due to its good conductivity, but it is not the case for the semiconducting ones, which therefore enable to identify metallic and semiconducting CNTs by the voltage contrast. So our first experiment is to apply a potential to the SWCNTs in SEM.

To apply a voltage on the CNT sample, we first deposited 10/50 nm thick Ti/Au electrodes to the ends of SWCNTs by electron beam evaporator (ANELVA L-400EK) and then put it on the sample stage of SEM. At least two neighboring electrodes were connected to a source meter (Keithley 2410) outside SEM chamber via electrical feedthroughs on a flange of SEM. In case of no voltage applied between two neighboring electrodes (corresponding to the normal SEM condition), as shown in Figure2b, there are apparent contrast differences for the observed SWCNTs. SWCNTs marked by S1, S2, S3, and S4 are much darker than those marked by T1, T2, T3, B1, B2, B3, C1, and C2. It is also clear from the SEM image that SWCNTs marked by S1, T1, T2, and T3 are only connected to the upper electrode, SWCNTs marked by S2, S3, S4, B1, B2, and B3 are only connected to the lower electrode, and SWCNTs marked by C1 and C2 are connected to both electrodes. Note that SWCNTs marked by T1 and C1 seem to be the same one tube but actually a bundle of two tubes. To help identifying the nanotubes, a schematic illustration was drawn in Figure 2a. When a potential of 15 V was applied between the two electrodes under SEM, as shown in Figure 2c, the upper electrode became darker because its higher voltage hindered the secondary electron emission from its surface. The SWCNTs connected to the upper electrode and marked by T1, T2, and T3 also became darker, which meant that their potential was the same as the upper electrode. SWCNTs marked by T1, T2, and T3 should possess good conductivity and therefore probably metallic. On the contrary, SWCNT marked by S1 was also connected to the upper electrode but did not become as dark as T1, T2, and T3. We therefore conclude that S1 possesses poor conductivity and is probably semiconducting. When the potential difference between the two electrodes was inversed, the brighter SWCNTs in Figure 2c (marked by B1, B2, and B3) became darker, and the darker SWCNTs (marked by T1, T2, and T3) became brighter in Figure2d. But there was no such contrast change for SWCNTs marked by S1, S2, S3, and S4. We can therefore conclude that SWCNTs marked by B1, B2, B3, T1, T2, and T3 are of good conductivity and probably metallic, and SWCNTs marked by

dx.doi.org/10.1021/nl301561f | *Nano Lett.* 2012, 12, 4095−4101

S1, S2, S3, and S4 are of poor conductivity and probably semiconducting. If we look carefully at the SWCNTs marked by C1 and C2 which were connected to both electrodes, there was a gradual contrast change from bright to dark along the tube as a voltage was applied. This gradual contrast change reflects a uniform potential distribution along the tube axis. Thus, these two SWCNTs should be of good conductivity. To sum up, with the help of voltage contrast SEM images (Figure 2c,d), the SWCNTs can be classified into two groups according to the conductivity difference: the good-conductivity group (marked by T1, T2, T3, B1, B2, B3, C1, and C2) and the poor-conductivity group (marked by S1, S2, S3, and S4). Note that the good-conductivity and poor-conductivity groups just correspond to the brighter and the darker SWCNTs in the normal SEM images (Figure 2b), respectively.

To directly verify whether the contrast difference in normal SEM images originates from the conductivity difference, the conductivity of SWCNTs was measured directly using peak force tunneling atom force microscopy (Peakforce TUNA, Bruker). As mentioned earlier, a 10/50 nm thick Ti/Au electrode was deposited onto the quartz substrate by electron beam evaporation to connect with the SWCNTs. A dc bias was applied between the AFM tip and the electrode, and then the current through tip−CNT−electrode was recorded when the tip was tapping on the CNT. As the voltage was fixed, the current should be proportional to the conductivity of the CNT. Normal AFM image, SEM image, and current image (from Peakforce TUNA) of four tubes (labeled as 1, 2, 3, and 4 from left to right) are shown in Figure 3, which demonstrate clearly

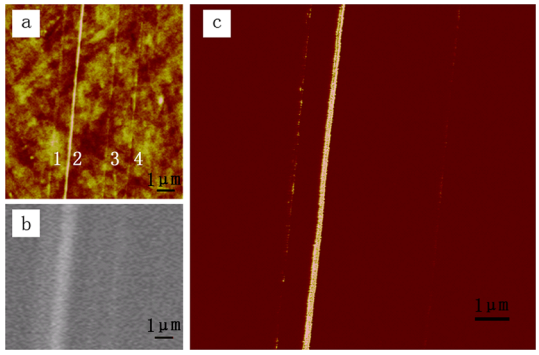

Figure 3. (a) Normal AFM image, (b) SEM image, and (c) current image measured by Peakforce TUNA for the same four tubes. The bright one acts more conductive, and it seems that little current goes through the two on the right. The scale bar is 1 μm.

the correlation between the contrast of SEM image and the current (or conductivity) of SWCNTs. The order of brightness is 2 > 1 > 4 > 3, and so is the conductivity. The relationship between the conductivity and the contrast is the same as the result of voltage contrast experiment. This is a very useful phenomenon as it points out directly the highly conductive or probably metallic carbon nanotube for its high brightness, and the dark ones can be inferred to be probably semiconducting. Many tubes have been measured, and this kind of correlation and identification method can be confirmed.

In aforementioned experiments, SWCNTs with good conductivity are probably metallic, but there is still possibility that they are on-state semiconducting SWCNTs. In case of the SWCNTs with poor conductivity, it does not imply semiconducting SWCNTs directly as well because there is also the possibility that the SWCNTs did not connected to the electrode properly. A bad connection will result in poor conductivity in the aforementioned experiments, even if the SWCNTs are metallic. To prove that the aforementioned good-conductivity and poor-conductivity SWCNTs are metallic and semiconducting respectively, further transfer characteristics measurements were carried out. Since it is relatively difficult to fabricate FET on quartz and keep the observability of CNTs, CNTs were transferred onto a Si wafer with a 500 nm thick SiO_2 top layer using a published transfer method.[24] Then arrays of FET devices were prepared on the SiO_2/Si substrate. One device sample is shown in Figure 4a. The electrodes are composed of a 10 nm Ti layer and 50 nm Au layer. CNTs which would not to be measured were etched away by O_2 plasma to make them electrically disconnected with the upper electrode. Figure 4b shows a typical testing result of the metallic SWCNT device shown in Figure 4a. The tube connected with electrodes in Figure 4a has bright contrast, and the supposed metallic character is confirmed clearly by the current−gate voltage (I_d−V_g) transfer characteristics measurement (Figure 4b). The ratio of maximum to minimum current in the curve is less than 3. For the device with multitubes, this identification method works well, too. In Figure 4c, three tubes connected with two electrodes appear a little darker, suggesting that they are all semiconducting. The I_d−V_g curve is plotted in Figure 4d, showing that no metallic tube exists exactly. The ON/OFF ratio of this FET device is over 10^3.

To go much further, some devices with both metallic and semiconducting carbon nanotubes were prepared, and the metallic ones were cut off by electrical breakdown[25] to compare their SEM images before and after breakdown. In Figure 5a, there was one bright tube on the left and one dark tube on the right connected with the electrodes. I_d−V_g curve measurement shows that there is at least one metallic tube (Figure 5d). Then the gate voltage was set as 2 V to keep the semiconducting tube off. As the drain voltage increased to about 80 V, one tube was electrically broke down (Figure 5b). Comparing the two SEM images (Figures 5a and 5c), we can find that the bright one on the left was cut off at two locations marked by the red circles in Figure 5c and the tube between two gaps became dark (which will be discussed later). I_d−V_g curve measurement after breakdown (Figure 5e) shows distinct semiconductivity of the right tube. This process demonstrates that the bright one is metallic and the dark one is semiconducting in the FET device very clearly.

The aforementioned experimental results indicate that the semiconducting and metallic SWCNTs can be directly identified in SEM by contrast difference. Now the question is why there is this kind of relationship between the types of SWCNTs and the contrast of SEM images.

Considering that difference in surface potential can induce so-called "voltage contrast"[23] which has been verified by *in situ* applying voltage across SWCNT samples, we therefore conjecture that the contrast difference in SEM images might originate from the difference in surface potentials.

It has been observed by many groups that SWCNTs on insulator surfaces can be imaged clearly with bright contrast by low-voltage SEM even though the diameters of SWCNTs are much smaller than the resolution of SEM.[26−33] Several mechanisms have been proposed for this phenomenon, such as the electron-beam-induced current (EBIC)[26] and voltage contrast for local potential difference.[27−29] All the proposed mechanisms share the same point that the bright contrast is due

dx.doi.org/10.1021/nl301561f | *Nano Lett.* 2012, 12, 4095−4101

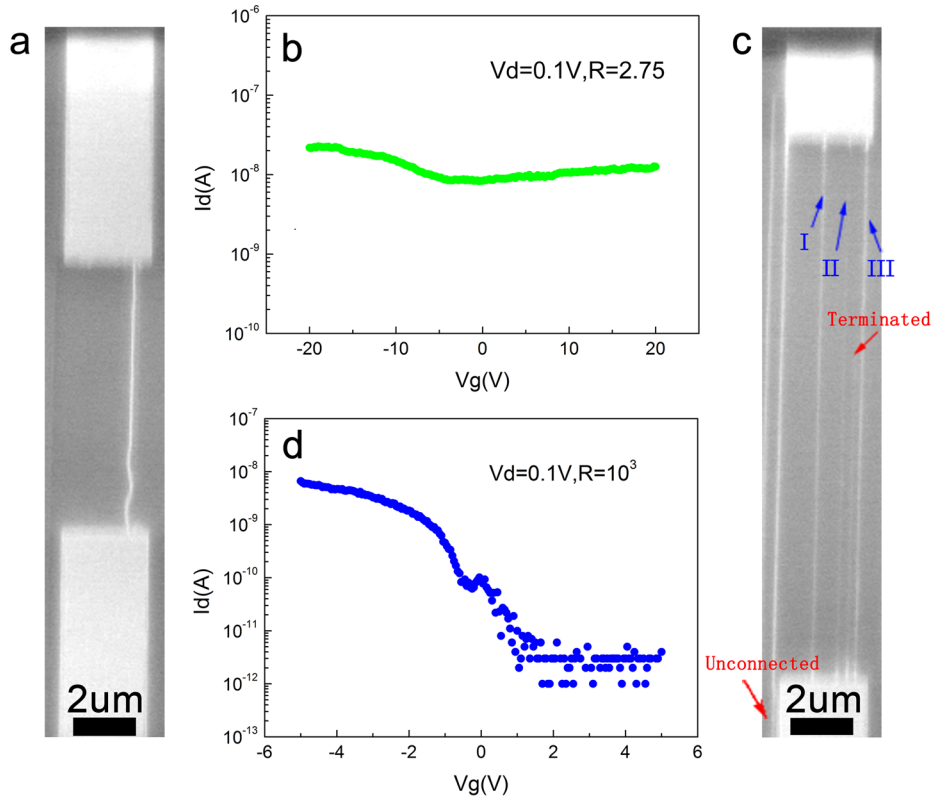

Figure 4. (a) SEM image of an FET device with one conductive carbon nanotube. The tube has same contrast with the electrodes. (b) I_d−V_g curve measurement of the device in (a). V_g was scanned from −20 to 20 V. R is the ratio of maximum to minimum current in the curve. The small R shows that this tube is metallic. (c) SEM image of an FET device with three tubes marked by the blue arrows, which are much darker than the electrodes. No metallic tube was found among them from the I_d−V_g curve measurement in (d). The ON/OFF ratio is over 10^3.

to the difference in the charging characteristics between SWCNTs and the insulator surface.

The charging of insulator surfaces under e-beam irradiation has been studied extensively in the past years.[23,34] For bulk insulators, when the e-beam energy is between tens of eV and tens of keV, its surface will be positively charged because the secondary electron emission coefficient $\sigma > 1$ which means the surface emits more secondary electrons than primary electrons that penetrated it. The surface potential is in the order of several volts. For a thin layer of SiO_2 over silicon substrate, its surface will be positively charged when the energy of e-beam is below 3 keV but negatively charged when the e-beam energy is above 3 keV, according to theoretical calculations.[30,35] Many experimental results agree well with this theoretical result. Note that the positive surface potential only exists in the area irradiated by e-beam. This can be easily verified by zooming out under SEM. The previously irradiated area appears as a dark rectangle in the new SEM image, due to the surface potential contrast. In our experiments, two kinds of SWCNT samples were used. The first kind is the as-grown SWCNT array on quartz substrate (Figure 1a). In this case the substrate is a bulk insulator, thus should be always positively charged when irradiated by e-beam with energies ranging from 1 to 10 keV. The second kind is the SWCNTs array transferred from quartz substrate onto SiO_2 (500 nm)/Si substrate (Figures 4 and 5). In this case, the surface is positively charged with beam energy from 1 to 3 keV and negatively charged with energy above 3 keV. Since the beam energy used was kept at 1 keV, the insulator surface is always positively charged in both cases.

Now considering those SWCNTs well contacted with the charging surface, if the metallic one is well electronically connected with the metal electrode (Figures 4 and 5) or other SWCNTs (Figure 1) out of the irradiated area which can act as an electron supply source, its potential will be the same as electrode outside irradiated area due to its good conductivity. There will be potential gradient between SWCNTs and the charging surface. Then electrons on the nanotube will spread into the surrounding surface, and the spreading range depends on the potential difference and the surface conductivity of the insulator. This process rebuilds the potential distribution and makes up the ultimate voltage contrast image (Figure 6). The positively charged substrate is dark, the SWCNT is bright, and the surrounding region is brighter than the rest of the surface, broadening the diameter of SWCNT to a much larger size at tens of nanometers.

In case that metallic SWCNTs were not well electronically connected with metal electrodes or other CNTs outside the irradiated area (such as the isolated SWCNT segment shown in Figure 5c), it possessed the same surface potential with the insulator surface. But it can still be distinguished from the substrate. This contrast might be originated from height difference, curvature difference, and difference in secondary electron emission coefficient.

Compared with the metallic SWCNT, the semiconducting one at off-state has poor conductivity and thus shows almost the same positive potential as the insulator surface even though it is connected with the metal electrodes or other CNTs outside the irradiated area. Therefore, it should have the same contrast as the isolated metallic SWCNTs (Figure 5c).

dx.doi.org/10.1021/nl301561f | *Nano Lett.* 2012, 12, 4095−4101

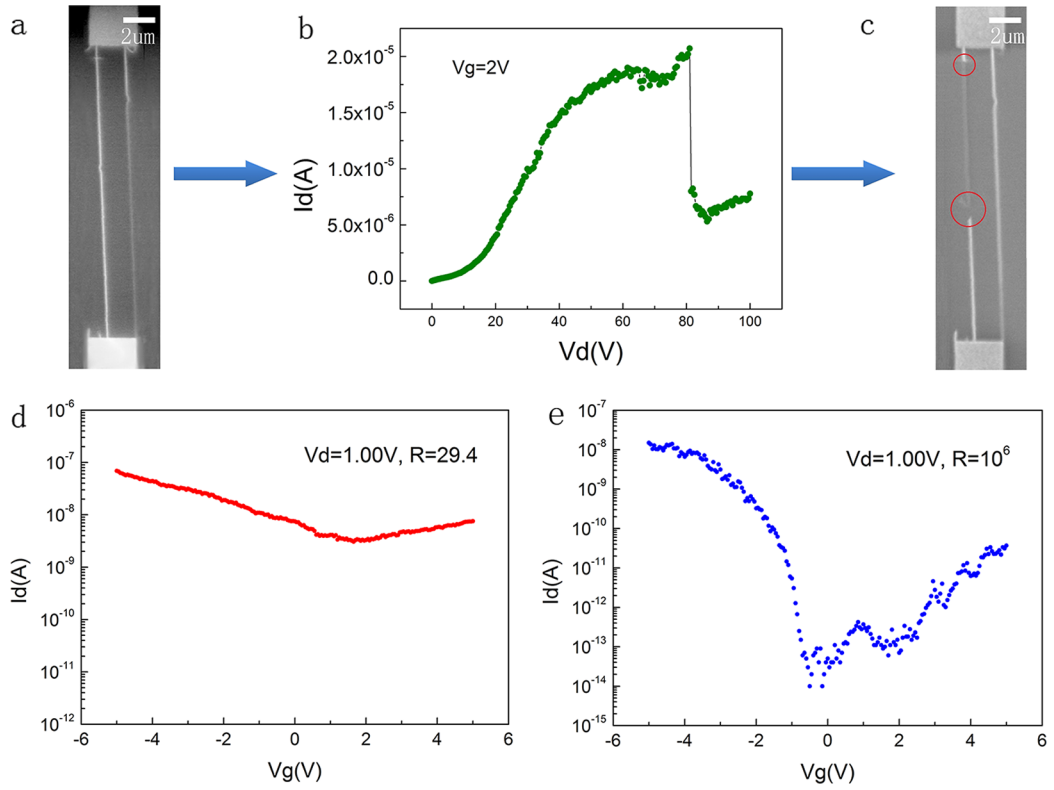

Figure 5. Electrical breakdown process. (a) SEM image of a FET device with two carbon nanotubes, appearing bright and dark from the left to the right. (b) A typical I_d–V_d curve of electrical breakdown. (c) SEM image after breakdown; the bright one has been broke down. (d) I_d–V_g curve measurement before breakdown. The ON/OFF ratio is lower than 50. (e) I_d–V_g curve measurement after breakdown, showing a typical ON/OFF ratio of 10^3–10^6.

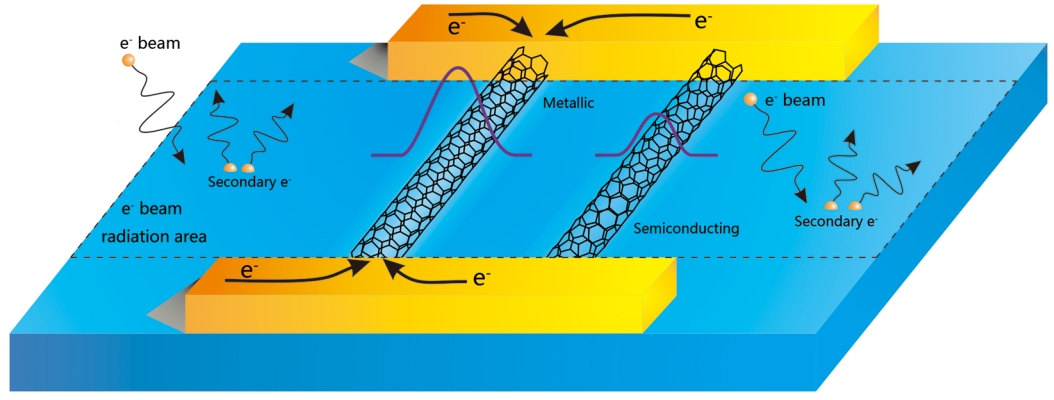

Figure 6. Schematic illustration of the origin of contrast difference between metallic and semiconducting SWCNTs. Because of its good conductivity, metallic SWCNTs can conduct more electrons from electrodes outside the e-beam irradiated area to the positively charged insulator surface than the semiconducting ones, resulting in the voltage contrast SEM image.

However, if we look at the SEM image shown in Figure 5c, the off-state semiconducting SWCNT connected to electrodes looks a little bit brighter than the isolated metallic SWCNT; this contrast difference might originate from the difference in secondary electron emission coefficient as well as a small fraction of voltage contrast due to the finite conductivity of off-state semiconducting SWCNTs.

Here we would like to stress that the contrast has a direct relationship with the conductivity according to the aforementioned discussion. Actually, the metallic nanotubes and semiconducting nanotubes at on-state both have good conductivity; they are both supposed to have bright contrast. However, we did not find semiconducting nanotubes with bright contrast in the experiments. A possible reason is that the as-grown semiconducting SWCNTs are p-type and are at off-state without gate voltage. Furthermore, the positively charged insulator surface will also apply a positive gate voltage to the SWCNTs and turn off the semiconducting SWCNTs. Hence, this identification method of metallic and semiconducting nanotubes works well here.

As a preliminary conclusion, the mechanism of the contrast difference between metallic and semiconducting SWCNTs involves three important parts: (1) the e-beam-irradiated insulator surface is positively charged; (2) the SWCNTs are connected to electrodes or other SWCNTs which are outside the irradiated area and can provide abundant electrons; (3) the

dx.doi.org/10.1021/nl301561f | *Nano Lett.* 2012, 12, 4095–4101

conductivity difference between metallic and semiconducting SWCNTs gives rise to different surface potential, resulting in a voltage contrast.

However, in the early papers,[26−28] researchers failed to find the contrast difference between the metallic and semiconducting SWCNTs. Now the question is why we succeed in identification of metallic and semiconducting SWCNTs in SEM. The necessary conditions for a successful identification in our experiments are shown here: (1) The SWCNTs should be connected to an electron reservoir located outside the irradiated area. In our as-grown sample on quartz substrate, the SWCNTs grown on the catalyst stripe is very dense, thus forming a natural electron reservoir. The stripe is centimeters long and thus obviously extrudes outside the irradiated area. An alternative way is to deposit long electrodes for SWCNTs, such as the electrodes we used for transferred SWCNTs on SiO_2/Si substrate, and make sure that the electrode is extending beyond the imaging area. (2) Since the contrast difference for metallic and semiconducting SWCNTs is relative observation and not huge, the metallic and semiconducting SWCNTs should appear in the same image for a direct comparison. Otherwise, one should keep the gray level of the insulator surface exactly identical, which is almost impossible for SEM imaging. (3) The SWCNTs should be in close contact with the insulator surface to form suitable surface potential distribution. If the SWCNT is suspended over or extruded outside the insulator surface, the height contrast plays the key role and thus metallic and semiconducting SWCNTs cannot be identified.

In conclusion, we have demonstrated that semiconducting and metallic single-walled carbon nanotubes on SiO_2, probably a variety of insulator substrates which were positively charged in low-voltage SEM, can have obviously different contrast in SEM and thus can be effectively and efficiently identified. This phenomenon can be understood via a proposed mechanism involving the e-beam-induced surface potential of insulators and the conductivity difference between metallic and off-state semiconducting SWCNTs.

Although we have demonstrated that SEM images can be used to identify semiconducting and metallic SWCNTs, there are still some challenges and drawbacks in this technology. (1) Since the contrast is a relative measure, it is easy to distinguish between two kinds of SWCNTs, but it is difficult to identify the property of an individual SWCNT. Hence, the challenge here is how to establish a standard to identify individual SWCNTs quantitatively in the future practical applications. How bright might a metallic tube be? How much darker might a semiconducting tube be than a metallic one? (2) As for further research, it is reasonable to expect that the semiconducting SWCNTs with different band gaps would have different appearance in the voltage-contrast picture, maybe just different contrast. If this is true, electronic structures of SWCNTs can be easily and directly obtained from a SEM contrast image, which provides a rapid technique for characterizing performance of SWCNT devices such as FETs. (3) This technology will not work if metallic and semiconducting carbon nanotubes twist together or are so close to each other to become a bundle in the image.

Despite these challenges and drawbacks, this method demonstrates great promise to achieve rapid and large-scale identification of metallic and semiconducting SWCNTs, adding a new function to conventional SEM.

AUTHOR INFORMATION

Corresponding Author

*Tel +86 10 62796017; fax +86 10 62792457; e-mail JiangKL@tsinghua.edu.cn.

Present Address

[†]Department of Materials Science and Engineering, University of California, Berkeley, CA 94720.

Notes

The authors declare no competing financial interest.

ACKNOWLEDGMENTS

This work was financially supported by the National Basic Research Program of China (2012CB932301), NSFC (50825201, 51102146, 90921012), and Fok Ying Tung Education Foundation (111049). We thank Hao Sun and Dengli Qiu from Nano Surface Instrumentation Group of Bruker for the help in peak force tunneling AFM.

REFERENCES

(1) Dresselhaus, M. S.; Dresselhaus, G.; Eklund, P. C. *Science of Fullerenes and Carbon Nanotubes*; Academic Press: San Diego, 1996.

(2) Saito, R.; Dresselhaus, G.; Dresselhaus, M. S.; et al. *Physical Properties of Carbon Nanotubes*; Imperial College Press: London, 1998; Vol. 3.

(3) Tans, S. J.; Devoret, M. H.; Dai, H.; Thess, A.; Smalley, R. E.; Geerligs, L. J.; Dekker, C. *Individual Single-Wall Carbon Nanotubes as Quantum Wires* **1997**, *386* (6624), 474−477.

(4) White, C. T.; Todorov, T. N. *Carbon Nanotubes as Long Ballist. Cond.* **1998**, *393* (6682), 240−242.

(5) Kong, J.; Yenilmez, E.; Tombler, T. W.; Kim, W.; Dai, H.; Laughlin, R. B.; Liu, L.; Jayanthi, C. S.; Wu, S. Y. Quantum Interference and Ballistic Transmission in Nanotube Electron Waveguides. *Phys. Rev. Lett.* **2001**, *87* (10), 106801.

(6) Close, G. F.; Yasuda, S.; Paul, B.; Fujita, S.; Wong, H. S. P. A 1 GHz Integrated Circuit with Carbon Nanotube Interconnects and Silicon Transistors. *Nano Lett.* **2008**, *8* (2), 706−709.

(7) Martel, R.; Schmidt, T.; Shea, H. R.; Hertel, T.; Avouris, P. Single- and multi-wall carbon nanotube field-effect transistors. *Appl. Phys. Lett.* **1998**, *73* (17), 2447−2449.

(8) Bachtold, A.; Hadley, P.; Nakanishi, T.; Dekker, C. *Logic Circuits Carbon Nanotube Transistors* **2001**, *294*, 1317−1320.

(9) Chen, Z. *Integr. Logic Circuit Assembled Single Carbon Nanotube* **2006**, *311*, 1735.

(10) Javey, A.; Tu, R.; Farmer, D. B.; Guo, J.; Gordon, R. G.; Dai, H. High Performance n-Type Carbon Nanotube Field-Effect Transistors with Chemically Doped Contacts. *Nano Lett.* **2005**, *5* (2), 345−348.

(11) Dresselhaus, M. S.; Dresselhaus, G.; Jorio, A.; Souza Filho, A. G.; Saito, R. Raman spectroscopy on isolated single wall carbon nanotubes. *Carbon* **2002**, *40* (12), 2043−2061.

(12) Jorio, A.; Saito, R.; Hafner, J. H.; Lieber, C. M.; Hunter, M.; McClure, T.; Dresselhaus, G.; Dresselhaus, M. S. Structural (n, m) Determination of Isolated Single-Wall Carbon Nanotubes by Resonant Raman Scattering. *Phys. Rev. Lett.* **2001**, *86* (6), 1118−1121.

(13) Gao, B.; Zhang, Y.; Zhang, J.; Kong, J.; Liu, Z. Systematic Comparison of the Raman Spectra of Metallic and Semiconducting SWNTs. *J. Phys. Chem. C* **2008**, *112* (22), 8319−8323.

(14) Bachtold, A.; Fuhrer, M. S.; Plyasunov, S.; Forero, M.; Anderson, E. H.; Zettl, A.; McEuen, P. L. Scanned Probe Microscopy of Electronic Transport in Carbon Nanotubes. *Phys. Rev. Lett.* **2000**, *84* (26), 6082−6085.

(15) Lu, W.; Xiong, Y.; Hassanien, A.; Zhao, W.; Zheng, M.; Chen, L. A Scanning Probe Microscopy Based Assay for Single-Walled Carbon Nanotube Metallicity. *Nano Lett.* **2009**, *9* (4), 1668−1672.

(16) Heo, J.; Bockrath, M. Local Electronic Structure of Single-Walled Carbon Nanotubes from Electrostatic Force Microscopy. *Nano Lett.* **2005**, *5* (5), 853−857.

(17) Kocabas, C.; Hur, S. H.; Gaur, A.; Meitl, M. A.; Shim, M.; Rogers, J. A. Guided Growth of Large-Scale, Horizontally Aligned Arrays of Single-Walled Carbon Nanotubes and Their Use in Thin-Film Transistors. *Small* **2005**, *1* (11), 1110−1116.
(18) Ding, L.; Yuan, D.; Liu, J. Growth of High-Density Parallel Arrays of Long Single-Walled Carbon Nanotubes on Quartz Substrates. *J. Am. Chem. Soc.* **2008**, *130* (16), 5428−5429.
(19) Ding, L.; Tselev, A.; Wang, J.; Yuan, D.; Chu, H.; McNicholas, T. P.; Li, Y.; Liu, J. Selective Growth of Well-Aligned Semiconducting Single-Walled Carbon Nanotubes. *Nano Lett.* **2009**, *9* (2), 800−805.
(20) Xiao, J.; Dunham, S.; Liu, P.; Zhang, Y.; Kocabas, C.; Moh, L.; Huang, Y.; Hwang, K.; Lu, C.; Huang, W.; Rogers, J. A. Alignment Controlled Growth of Single-Walled Carbon Nanotubes on Quartz Substrates. *Nano Lett.* **2009**, *9* (12), 4311−4319.
(21) Ishikawa, F. N.; Chang, H.; Ryu, K.; Chen, P.; Badmaev, A.; Gomez De Arco, L.; Shen, G.; Zhou, C. Transparent Electronics Based on Transfer Printed Aligned Carbon Nanotubes on Rigid and Flexible Substrates. *ACS Nano* **2009**, *3* (1), 73−79.
(22) Li, Y.; Cui, R.; Ding, L.; Liu, Y.; Zhou, W.; Zhang, Y.; Jin, Z.; Peng, F.; Liu, J. *How Catalysts Affect the Growth of Single-Walled Carbon Nanotubes on Substrates*; Wiley-VCH Verlag: Berlin, 2010; Vol. *22*, pp 1508−1515.
(23) Wells, O. C. *Scanning Electron Microscopy*; McGraw-Hill: New York, 1974.
(24) Jiao, L.; Fan, B.; Xian, X.; Wu, Z.; Zhang, J.; Liu, Z. Creation of Nanostructures with Poly(methyl methacrylate)-Mediated Nanotransfer Printing. *J. Am. Chem. Soc.* **2008**, *130* (38), 12612−12613.
(25) Collins, P. G.; Arnold, M. S.; Avouris, P. Engineering Carbon Nanotubes and Nanotube Circuits Using Electrical Breakdown. *Science* **2001**, *292* (5517), 706−709.
(26) Homma, Y.; Suzuki, S.; Kobayashi, Y.; Nagase, M.; Takagi, D. Mechanism of bright selective imaging of single-walled carbon nanotubes on insulators by scanning electron microscopy. *Appl. Phys. Lett.* **2004**, *84*, 1750.
(27) Brintlinger, T.; Chen, Y. F.; D U Rkop, T.; Cobas, E.; Fuhrer, M. S.; Barry, J. D.; Melngailis, J. Rapid imaging of nanotubes on insulating substrates. *Appl. Phys. Lett.* **2002**, *81*, 2454.
(28) Zhang, R. Y.; Wei, Y.; Nagahara, L. A.; Amlani, I.; Tsui, R. K. The contrast mechanism in low voltage scanning electron microscopy of single-walled carbon nanotubes. *Nanotechnology* **2006**, *17*, 272.
(29) Croitoru, M.; Bertsche, G.; Kern, D. P.; Burkhardt, C.; Bauerdick, S.; Sahakalkan, S.; Roth, S. Visualization and in situ contacting of carbon nanotubes in a scanning electron microscope. *J. Vac. Sci. Technol., B* **2005**, *23*, 2789−2792.
(30) Finnie, P.; Kaminska, K.; Homma, Y.; Guy Austing, D.; Lefebvre, J. Charge contrast imaging of suspended nanotubes by scanning electron microscopy. *Nanotechnology* **2008**, *19*, 335202.
(31) Zhou, Y. S.; Yi, K. J.; Mahjouri-Samani, M.; Xiong, W.; Lu, Y. F.; Liou, S. H. Image contrast enhancement in field-emission scanning electron microscopy of single-walled carbon nanotubes. *Appl. Surf. Sci.* **2009**, *255* (7), 4341−4346.
(32) Zhang, L.; Gao, F.; Huang, S. The imaging mechanism of single-walled carbon nanotubes on Si/SiO_2 wafer in scanning electron microscopy. *J. Microsc.* **2011**, *241* (2), 188−194.
(33) Vijayaraghavan, A.; Blatt, S.; Marquardt, C.; Dehm, S.; Wahi, R.; Hennrich, F.; Krupke, R. Imaging electronic structure of carbon nanotubes by voltage-contrast scanning electron microscopy. *Nano Res.* **2008**, *1* (4), 321−332.
(34) Seah, M. P.; Spencer, S. J. AES of bulk insulators − control and characterisation of the surface charge. *J. Electron Spectrosc. Relat. Phenom.* **2000**, *109* (3), 291−308.
(35) Glavatskikh, I. A.; Kortov, V. S.; Fitting, H. J. Self-consistent electrical charging of insulating layers and metal-insulator-semiconductor structures. *J. Appl. Phys.* **2001**, *89*, 440.